

Nuclear double resonance: Cross relaxation rates between two spin species*

Harold T. Stokes and David C. Ailion

Department of Physics, University of Utah, Salt Lake City, Utah 84112

(Received 30 August 1976)

A rotating-frame nuclear-double-resonance experiment is reported in which the cross-relaxation rates between ${}^7\text{Li}$ and ${}^6\text{Li}$ in powdered lithium metal were measured. The theory developed by McArthur, Hahn, and Walstedt (MHW) is applied to these data and good agreement is obtained. We also apply this theory to other published experimental data (LiF by Lang and Moran and adamantane by Pines and Shattuck) and find good agreement. We conclude that the assumption of a Lorentzian correlation function, which forms the basis of the theory of MHW, is generally valid.

I. INTRODUCTION

Nuclear-double-resonance spectroscopy is now a well-known technique for studying nuclei whose NMR signals are too weak to be detected directly. This technique depends upon cross relaxation between two spin species, one abundant (hereafter referred to as I spins) and one dilute (hereafter referred to as S spins).

McArthur, Hahn, and Walstedt¹ (MHW) carefully measured cross-relaxation rates between ${}^{19}\text{F}$ (I spins) and ${}^{43}\text{Ca}$ (S spins) in CaF_2 under various experimental conditions. In particular, they treated the case of adiabatic demagnetization in the rotating frame in which the I spins were in the demagnetized state and the S spins were irradiated by an rf field near their resonant frequency. Using a thermodynamic model and assuming a Lorentzian correlation function for the dipolar fluctuations, they formed a theory which successfully fit the data.

Demco, Tegenfeldt, and Waugh² (DTW) refined this theory, using a more fundamental approach involving memory functions. This theory, when applied to the CaF_2 work of MHW,¹ resulted in a slight improvement in the agreement between data and theory. But, on the whole, the DTW and MHW theories were shown to be in close agreement for the case of CaF_2 . It is unknown whether or not this close agreement also exists in other cases.

In this paper, we examine the MHW theory, applying it to other cases and comparing it to available data. We will show that this theory seems to be generally adequate for calculating cross relaxation rates, which is fortunate since calculations using the DTW theory are much more lengthy than those using the theory of MHW.

II. THEORY

Consider a system of two spin species, I spins and S spins. The I spins are in a state of dipolar order (see Sec. III in this paper) and the S spins

are irradiated by an rf field H_{1S} at their resonant frequency.

Using a thermodynamic model, we describe the two sets of spin species with spin temperatures, β_I and β_S . Dipolar I - S interactions cause the system to cross relax towards a common temperature. From conservation of energy we have

$$\frac{d\beta_I}{dt} + \epsilon \frac{d\beta_S}{dt} = 0, \quad (1)$$

where the ratio of heat capacities ϵ of the two sets of spin species is given by^{1,2}

$$\epsilon = N_S S(S+1) \gamma_S^2 H_{1S}^2 / N_I I(I+1) \gamma_I^2 H_{1I}^2. \quad (2)$$

Following a convention used by others^{1,2} we introduce a cross-relaxation rate τ_{CR}^{-1} which characterizes the relaxation of the S spins toward the common temperature. It is defined by the following equation:

$$\frac{d\beta_S}{dt} = -\tau_{\text{CR}}^{-1} (\beta_S - \beta_I). \quad (3)$$

Then

$$\frac{d\beta_I}{dt} = -\epsilon \tau_{\text{CR}}^{-1} (\beta_I - \beta_S). \quad (4)$$

To obtain a quantitative expression for τ_{CR}^{-1} , we follow MHW and write the Hamiltonian in the double rotating reference frame. Expressing the Hamiltonian in units of frequency, we obtain

$$\mathcal{H} = \mathcal{H}_{dII}^0 + \mathcal{H}_{dIS} + \mathcal{H}_{dIS}^0, \quad (5)$$

$$\mathcal{H}_{dII}^0 = \frac{1}{2} \sum_{i,k} A_{ik} (3I_{zi} I_{zk} - \vec{I}_i \cdot \vec{I}_k), \quad (6)$$

$$\mathcal{H}_{dIS} = -\gamma_S H_{1S} \sum_k S_{zk}, \quad (7)$$

$$\mathcal{H}_{dIS}^0 = \sum_{i,k} B_{ik} I_{zi} S_{zk}, \quad (8)$$

$$A_{ik} = \frac{1}{2} \gamma_I^2 \hbar \gamma_{ik}^{-3} (1 - 3 \cos^2 \theta_{ik}), \quad (9)$$

and

$$B_{ik} = \gamma_I \gamma_S \bar{n} \gamma_{ik}^{-3} (1 - 3 \cos^2 \theta_{ik}), \quad (10)$$

where a coordinate system has been chosen with \bar{H}_0 along the z axis and \bar{H}_{1S} along the x axis. As in MHW's paper, we assume that dipolar interactions between the dilute S spins can be neglected.

We then assign spin temperature β_I and β_S to the terms \mathcal{H}_{dII}^0 and \mathcal{H}_{zS} respectively and write the density matrix as

$$\sigma = 1 - \beta_I \mathcal{H}_{dII}^0 - \beta_S \mathcal{H}_{zS}. \quad (11)$$

Treating \mathcal{H}_{dIS}^0 as a perturbation which causes β_I and β_S to evolve with time towards a common value, we obtain, using perturbation theory,¹ for H_{1S} on resonance,

$$\tau_{CR}^{-1} = \langle \Delta\omega^2 \rangle_{SI} J(\gamma_S H_{1S}), \quad (12)$$

where

$$J(\omega) = \int_0^\infty d\tau \cos(\omega\tau) G(\tau), \quad (13)$$

$$G(\tau) = \text{tr}[\mathcal{H}_{dIS}^0(\tau) \mathcal{H}_{dIS}^0] / \text{tr}(\mathcal{H}_{dIS}^0)^2, \quad (14)$$

and

$$\mathcal{H}_{dIS}^0(\tau) = \exp(i\tau \mathcal{H}_{dII}^0) \mathcal{H}_{dIS}^0 \exp(-i\tau \mathcal{H}_{dII}^0). \quad (15)$$

The term $\langle \Delta\omega^2 \rangle_{SI}$ is the Van Vleck second moment of the S spins' NMR line due to I - S dipolar interactions³ and is given by

$$\langle \Delta\omega^2 \rangle_{SI} = \frac{1}{3} I(I+1) \sum_j B_{jm}^2. \quad (16)$$

In order for this perturbation method to be valid, the rf field H_{1S} must be large. This comes from two different considerations. First, the "heat capacity" of \mathcal{H}_{zS} must be larger than that of \mathcal{H}_{dIS}^0 ; that is, the perturbation must be small compared to either of the other two parts of the Hamiltonian. This condition can be written

$$\gamma_S^2 H_{1S}^2 \gg \langle \Delta\omega^2 \rangle_{SI}. \quad (17)$$

Second, we must have "fast correlation." This means that the correlation function $G(\tau)$ must decay to zero much quicker than the time evolution of the density matrix. This can be written

$$\tau_C \ll \tau_{CR}, \quad (18)$$

where τ_C is the correlation time of $G(\tau)$. Since τ_{CR} increases with increasing H_{1S} , this condition restricts H_{1S} to large values.

At this point, it should be noted that the description of the S spins with a spin temperature β_S is actually invalid. The S - S interactions are too weak to maintain a Boltzmann distribution among the energy levels of \mathcal{H}_{zS} . We can, nevertheless, *define* thermodynamic variables, β_I and β_S , by the following

expression:

$$\beta_I \equiv \langle \mathcal{H}_{dII}^0 \rangle / \text{tr}(\mathcal{H}_{dII}^0)^2, \quad (19)$$

$$\beta_S \equiv \langle \mathcal{H}_{zS} \rangle / \text{tr}(\mathcal{H}_{zS})^2. \quad (20)$$

If we then proceed to use perturbation theory, assuming a Boltzmann distribution only among the energy levels of \mathcal{H}_{dII}^0 , we obtain the same results, as was shown in detail by DTW.²

In order to evaluate τ_{CR}^{-1} , it is necessary to calculate the correlation function $G(\tau)$. Since $G(\tau)$ cannot be calculated exactly, an approximation must be used. This is where the MHW and DTW theories differ. The DTW theory involves a memory function which uses both the second and fourth moments of $J(\omega)$ to generate $G(\tau)$. The MHW theory, on the other hand, assumes the form of $G(\tau)$ to be Lorentzian (as will be explained in more detail below) and consequently uses only the second moment of $J(\omega)$. Thus, the DTW theory is probably more accurate and more generally applicable to different situations. The DTW theory suffers a major disadvantage, though. The numerical calculations are long and tedious, involving several double and triple lattice sums, as well as numerical integration. One would hope that a simplifying assumption could be made to reduce the numerical work without greatly destroying the accuracy. Such is the case with the MHW theory.

From data taken on CaF_2 , MHW found τ_{CR}^{-1} to be exponential in H_{1S} . From Eq. (13) we can see that a Lorentzian correlation function would produce such a result. Thus, we try

$$G(\tau) = [1 + (\tau/\tau_C)^2]^{-1}. \quad (21)$$

From Eqs. (12) and (13), we then obtain¹

$$\tau_{CR}^{-1} = \frac{1}{2} \pi \langle \Delta\omega^2 \rangle_{SI} \tau_C \exp(-\gamma_S H_{1S} \tau_C). \quad (22)$$

By expanding both Eqs. (14) and (21) in powers of τ , we have

$$1 + \frac{1}{2} \tau^2 \left(\frac{d^2 G(\tau)}{d\tau^2} \right) \Big|_{\tau=0} + \dots = 1 - \left(\frac{\tau}{\tau_C} \right)^2 + \dots. \quad (23)$$

Equating the coefficients of τ^2 on both sides of the equation, we obtain an expression for τ_C :

$$1/\tau_C^2 = -\frac{1}{2} \text{tr}[\mathcal{H}_{dII}^0, \mathcal{H}_{dIS}^0]^2 / \text{tr}(\mathcal{H}_{dIS}^0)^2. \quad (24)$$

Evaluating the traces, we obtain

$$1/\tau_C^2 = \frac{1}{9} \langle \Delta\omega^2 \rangle_{II} K, \quad (25)$$

where $\langle \Delta\omega^2 \rangle_{II}$ is the Van Vleck second moment of the I spins' NMR line due to I - I dipolar interactions and is given by

$$\langle \Delta\omega^2 \rangle_{II} = 3I(I+1) \sum_j A_{ij}^2. \quad (26)$$

The term K is a geometric factor given by

$$K = \left(\sum_{i,j} A_{ij}^2 (B_{jm}^2 - B_{im} B_{jm}) \right) / \left(\sum_j A_{ij}^2 \right) \left(\sum_j B_{jm}^2 \right). \quad (27)$$

In ionic crystals with cubic symmetry (sc, bcc, fcc, etc.), we have found the value of K to vary between about 0.5 and 1.0.

As an example, consider CaF_2 . The ^{19}F sublattice is simple cubic. We can write

$$\sum_j A_{ij}^2 = \gamma_I^4 \hbar^2 a_0^{-6} S_1(\text{sc}), \quad (28)$$

where

$$S_1(\text{sc}) = \sum_i \left(\frac{a_0}{r_{ik}} \right)^6 [P_2(\cos\theta_{ik})]^2 \quad (29)$$

and the summation is over a simple cubic lattice. Similarly,

$$\sum_j B_{jm}^2 = 4\gamma_I^2 \gamma_S^2 \hbar^2 a_0^{-6} S_1(\text{sc}'), \quad (30)$$

where the primed notation $S_1(\text{sc}')$ is a special case of Eq. (29) in which the index i is summed over the ^{19}F sublattice and k refers to a ^{43}Ca site—that is, a summation over a simple cubic lattice from a point not on the lattice. We can also write

$$\sum_{i,j} A_{ij}^2 B_{jm}^2 = 4\gamma_I^6 \gamma_S^2 \hbar^4 a_0^{-12} S_1(\text{sc}) S_1(\text{sc}') \quad (31)$$

and

$$\sum_{i,j} A_{ij}^2 B_{im} B_{jm} = 4\gamma_I^6 \gamma_S^2 \hbar^2 a_0^{-12} S_3(\text{sc}'), \quad (32)$$

where

$$S_3(\text{sc}') = \sum_{i,j} \left(\frac{a_0}{r_{ik}} \right)^3 \left(\frac{a_0}{r_{jk}} \right)^3 \left(\frac{a_0}{r_{ij}} \right)^6 \\ \times P_2(\cos\theta_{ik}) P_2(\cos\theta_{jk}) [P_2(\cos\theta_{ij})]^2. \quad (33)$$

As before, the primed notation $S_3(\text{sc}')$ refers to the case in which both indices i and j are summed over ^{19}F sublattice sites and k again represents a ^{43}Ca site. Finally, we can write for CaF_2 ,

$$1/\tau_C^2 = \frac{1}{3} I(I+1) \gamma_I^4 \hbar^2 a_0^{-6} S_1(\text{sc}) \\ \times [1 - S_3(\text{sc}')/S_1(\text{sc}) S_1(\text{sc}')]. \quad (34)$$

More details are given about these lattice sums in Appendix A.

At this point, it might be well to discuss the physical meaning of $G(\tau)$. On inspection of Eq. (14), we note that $G(\tau)$ has a mathematical form similar to that of the envelope of a normal free induction decay (FID):

$$G_{\text{FID}}(\tau) = \text{tr}[I_x(\tau)I_x]/\text{tr}(I_x)^2, \quad (35)$$

$$I_x(\tau) = \exp(i\tau \mathcal{H}_{dII}^0) I_x \exp(-i\tau \mathcal{H}_{dII}^0). \quad (36)$$

In a free induction decay, the x component of the magnetization (represented by $\langle I_x \rangle$) oscillates with frequency $\gamma_I H_0$ and is dephased by \mathcal{H}_{dII}^0 to zero in a time of the order of T_2 . The envelope of the decay of $\langle I_x \rangle$ is given by $G_{\text{FID}}(\tau)$. Similarly, in the cross-relaxation experiment, $\langle \mathcal{H}_{dIS}^0 \rangle$ oscillates with frequency $\gamma_S H_{1S}$ (in the rotating reference frame) and is dephased by \mathcal{H}_{dII}^0 to zero in a time of the order of τ_C . The envelope of the decay of $\langle \mathcal{H}_{dIS}^0 \rangle$ is given by $G(\tau)$. Such transient oscillations were observed by MHW.¹

As was noted earlier, the agreement between the MHW theory and experimental data for CaF_2 is very good.¹ There remains a question concerning the simplifying assumption of a Lorentzian correlation function. Is this assumption valid in cases other than CaF_2 ? In a few cases, experimental evidence^{4,5} has shown this to be the case. In this paper we will apply the MHW theory to other experimental data, thereby demonstrating the validity of using a Lorentzian correlation function in all cases studied.

III. EXPERIMENTAL PROCEDURES

At this point, we will outline the experimental procedures we use to measure τ_{CR} . We use a pulse technique, very similar to that of MHW,¹ shown in Fig. 1. The I spins are prepared in the demagnetized state by spin locking (that is, a 90° pulse followed by a 90° phase shift) and then adiabatic demagnetization.⁶ The S spins are then irradiated by N rf pulses, each of length τ_{ON} and separated by $\tau_{\text{OFF}} \gg T_{2S}$, the spin-spin relaxation time of the S spins.

Solving Eqs. (3) and (4) with the initial condition $\beta_S = 0$ at the beginning of each pulse gives the results of MHW for the case of negligible spin-lattice relaxation:

$$\frac{M_I(\tau_{\text{ON}})}{M_I(0)} = \frac{\beta_I(\tau_{\text{ON}})}{\beta_I(0)} \\ = \left(\frac{1 + \epsilon \exp\{-(1 + \epsilon)/\tau_{\text{CR}}\} \tau_{\text{ON}}}{1 + \epsilon} \right)^N. \quad (37)$$

To monitor β_I , we simply remagnetize the I spins⁶ and observe the free induction decay, whose amplitude M_I is proportional to β_I . Thus, for a given H_{1S} , we measure M_I for several values of τ_{ON} (including $\tau_{\text{ON}} = 0$) and then apply Eq. (37) to obtain τ_{CR} .

The amplitude of the rf field H_{1S} is measured using rotary saturation¹ (see Fig. 1). With the I spins in the demagnetized state, we apply a single long pulse of H_{1S} whose frequency is modulated by an audio frequency ω_a of small amplitude. This produces an effective modulation of H_0 which "heats" up the S spins.⁷ This effect is greatest

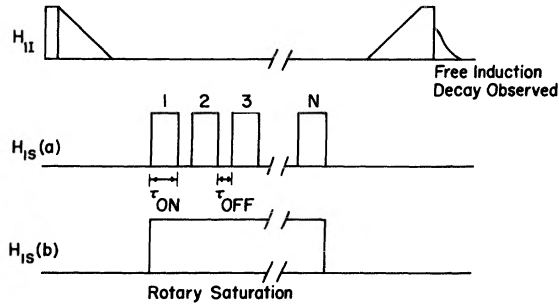


FIG. 1. Pulse sequence used for (a) measuring cross-relaxation rates, and (b) measuring the amplitude of H_{1S} .

at $\omega_a = \gamma_S H_{1S}$ (see Fig. 2), and thus enables us to obtain the amplitude of H_{1S} .

IV. EXPERIMENTAL RESULTS IN LITHIUM

We measured cross relaxation rates in powdered lithium metal ($I = {}^7\text{Li}$; $S = {}^6\text{Li}$). We used a sample of lithium-metal dispersion (30% lithium, 70% petroleum) manufactured by the Lithium Corp. of America, Inc. The sample was submerged in liquid nitrogen and placed in a dc magnetic field of approximately 14.5 kG. Under these conditions, we measured for ${}^7\text{Li}$ a spin-lattice relaxation time $T_1 = 574 \pm 10$ msec at 24 MHz and a dipolar relaxation time $T_{1D} = 300 \pm 10$ msec (cf., the results obtained by Ailion and Slichter⁸ who measured $T_1 = 470 \pm 14$ msec in another lithium sample at 7.5 MHz at the same temperature).

We measured the cross-relaxation rate at three

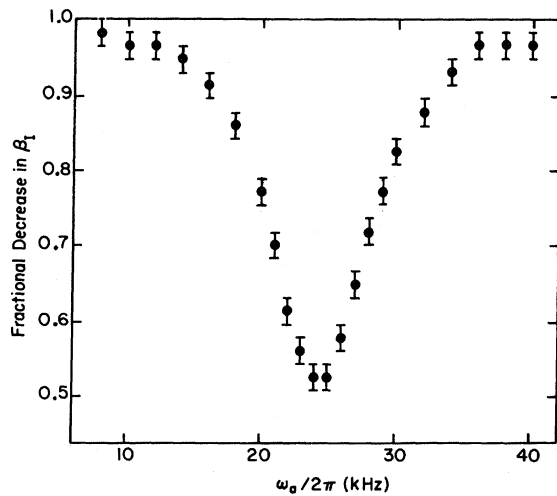


FIG. 2. Fractional decrease of β_I as a function of $\omega_a/2\pi$ using rotary saturation. This is an example of how H_{1S} can be measured. In this case we obtain $H_{1S} = 3.9 \pm 0.1$ G.

different values of H_{1S} (see Fig. 3). In doing this, we found that the experimental values of ϵ were consistent with a higher local field H_{LI} than the calculated dipolar local field (see Appendix B for further discussion of this point). Accordingly, we used the experimentally determined value of ϵ in determining τ_{CR}^{-1} from Eq. (37).

In applying the MHW theory to a powdered sample, one must recognize that each crystallite in the sample contributes to the magnetization independently of every other crystallite in the sample. To interpret experimental data, we must write the observed magnetization, given by Eq. (37) as a function of crystal orientation, and then average over all orientations⁹⁻¹¹:

$$M_{\text{obs}} = \langle M \rangle = \frac{1}{4\pi} \int_0^\pi \sin\theta d\theta \int_0^{2\pi} d\phi M(\theta, \phi). \quad (38)$$

Expressions for $M(\theta, \phi)$ can be written using angular dependences of the various lattice sums involved (see Appendix A), but it is immediately obvious that the integral in Eq. (38) cannot be evaluated analytically. An approximation to Eq. (38) may be obtained by replacing each individual lattice sum involved by its powder average. In the case of powdered lithium metal, we evaluated Eq. (38) numerically and found the error of this

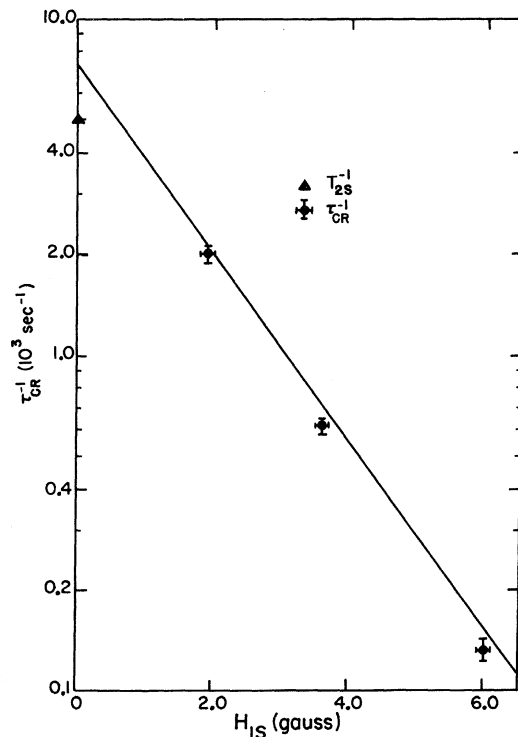


FIG. 3. Cross-relaxation rates in powdered lithium metal. The solid line is calculated from the MHW theory.

approximation to be less than 5%.

In Fig. 3, the experimental data is compared to the MHW theory (using the approximation described above). As can be seen, the agreement is quite good. A correlation time τ_C of 163 μ sec was calculated in this case, using

$$\frac{1}{\tau_C^2} = \frac{1}{3} I(I+1) \gamma_I^4 \hbar^2 a_0^{-6} \frac{N_I}{N_I + N_S} \times \langle S_1(\text{bcc}) \rangle \left(1 - \frac{\langle S_2(\text{bcc}) \rangle + \langle S_3(\text{bcc}) \rangle}{\langle S_1(\text{bcc}) \rangle^2} \right), \quad (39)$$

where the powder averages of S_1 , S_2 , and S_3 in a bcc lattice are denoted by $\langle S_1(\text{bcc}) \rangle$, $\langle S_2(\text{bcc}) \rangle$, and $\langle S_3(\text{bcc}) \rangle$, respectively. S_1 and S_3 have been defined earlier in Eqs. (29) and (33), respectively. S_2 is defined as

$$S_2 = \sum_i \left(\frac{a_0}{r_{ik}} \right)^{12} [P_2(\cos\theta_{ik})]^4. \quad (40)$$

Note that, by definition, the terms S_1 , S_2 , and S_3 are sums over *all* lattice sites, not just occupied sites. The terms which appear in Eq. (27), however, are sums over pairs of atoms and must be converted to sums over sites in order to be expressed as functions of S_1 , S_2 , and S_3 . In the case of CaF_2 , the sum over sites was identical to the sum over atoms; however, in metallic lithium, both I and S spins range over the same lattice so that these sums are not identical. The extra term S_2 arises from this feature as can be seen by considering the following term from Eq. (27), which will now be converted from a sum over atoms to a sum over sites:

$$\sum_{\substack{\text{atoms} \\ i, j}} A_{ij}^2 B_{jm}^2 = P_i P_j \sum_{\substack{\text{sites} \\ i, j}} A_{ij}^2 B_{jm}^2, \quad (41)$$

where P_i and P_j are the probabilities that sites i and j , respectively, are occupied by I spins. Since m is, by definition, an S site, $P_m = 0$. Thus

$$\left(\frac{1}{\tau_C^2} \right)_{6_{\text{Li}}-7_{\text{Li}}} = \frac{1}{3} I(I+1) \gamma_I^4 \hbar^2 a_0^{-6} \frac{N_I}{N_I + N_S} S_1(\text{fcc}) \left(1 - \frac{S_2(\text{fcc}) + S_3(\text{fcc})}{S_1(\text{fcc})^2} \right), \quad (45)$$

$$\left(\frac{1}{\tau_C^2} \right)_{6_{\text{Li}}-19_{\text{F}}} = \frac{1}{3} I(I+1) \gamma_I^4 \hbar^2 a_0^{-6} S_1(\text{fcc}) \left(1 - \frac{S_3(\text{fcc}')}{S_1(\text{fcc}) S_1(\text{fcc}')} \right), \quad (46)$$

where I refers to ${}^7\text{Li}$ in Eq. (45) and to ${}^{19}\text{F}$ in Eq. (46). The primed notation fcc' refers to summations between two different sublattices, as in the case of CaF_2 previously discussed. These correlation times are listed in Table I for three different crystal orientations. Values for τ_{CR}^{-1} using Eqs. (44) and (22) are shown in Fig. 4.

Data was published¹² only for \bar{H}_0 in the [111] di-

$$P_i = \begin{cases} N_I / (N_I + N_S), & i \neq m, \\ 0, & i = m. \end{cases} \quad (42)$$

This results in

$$\sum_{i, j} A_{ij}^2 B_{jm}^2 = 4 \gamma_I^6 \gamma_S^2 \hbar^4 a_0^{-12} \left(\frac{N_I}{N_I + N_S} \right)^2 \times [S_1^2(\text{bcc}) - S_2(\text{bcc})]. \quad (43)$$

Substituting the above and similar expressions in Eq. (27), we obtain Eq. (39).

V. COMPARISON WITH OTHER PUBLISHED RESULTS

A. Lithium fluoride

Lang and Moran¹² reported measurements in LiF ($I = {}^7\text{Li}$; $S = {}^6\text{Li}$). They observed that the cross relaxation rate as a function of H_{1S} has wings characteristic of a Lorentzian or exponential dependence on H_{1S} . This, of course, is consistent with the MHW theory. There is an additional complication in this case, though: a third spin species ${}^{19}\text{F}$. The ${}^6\text{Li}$ nuclei, irradiated by a strong rf field H_{1S} , cross relaxes with both the ${}^7\text{Li}$ and ${}^{19}\text{F}$ nuclei simultaneously. Under these conditions, fortunately, the ${}^7\text{Li}$ and ${}^{19}\text{F}$ nuclei cross relax much more rapidly with each other than either does with ${}^6\text{Li}$.

In other words, the ${}^7\text{Li}$ and ${}^{19}\text{F}$ nuclei maintain a common spin temperature in the rotating reference frame (this time rotating with respect to ${}^{19}\text{F}$ as well as ${}^7\text{Li}$ and ${}^6\text{Li}$). Such an assumption has been shown to be valid experimentally.^{13,14} We thus have, as suggested by DTW,²

$$1/\tau_{\text{CR}} = (1/\tau_{\text{CR}})_{6_{\text{Li}}-7_{\text{Li}}} + (1/\tau_{\text{CR}})_{6_{\text{Li}}-19_{\text{F}}}. \quad (44)$$

The correlation times of these two sets of interactions are given by

rection. Good agreement is found between this data and the MHW theory (see Fig. 4). But Lang and Moran¹² also reported that their measurements for the [110] and [100] orientations showed that τ_{CR}^{-1} increases over the [111] values an average of about 15 and 30% for the [110] and [100] directions, respectively. As can be seen in Fig. 4, this agrees qualitatively but disagrees quantitatively with the MHW theory

TABLE I. Correlation times τ_C given by Eqs. (45) and (46) for the ${}^6\text{Li}$ - ${}^7\text{Li}$ cross relaxation and for the ${}^6\text{Li}$ - ${}^{19}\text{F}$ cross relaxation with three different orientations of \vec{H}_0 in a single crystal of LiF.

Interaction pair	Orientation of \vec{H}_0		
	[100]	[110]	[111]
${}^6\text{Li}$ - ${}^7\text{Li}$	154 μsec	132 μsec	117 μsec
${}^6\text{Li}$ - ${}^{19}\text{F}$	49.5	41.9	45.2

which predicts increases of as much as an order of magnitude and more. There seems to be some limiting process in the sample which doesn't allow the cross relaxation to proceed as quickly as the theory would predict.

B. Adamantane

Pines and Shattuck⁴ reported measurements in polycrystalline adamantane ($I = {}^1\text{H}$; $S = {}^{13}\text{C}$). They found the cross-relaxation rate to be exponential in H_{1S} , consistent with the MHW theory.

Adamantane ($\text{C}_{10}\text{H}_{16}$) is a cage-like molecule which, at room temperature, sits in a face-centered-cubic lattice.¹⁵ If we were to calculate the cross-relaxation rates for a rigid lattice, we would obtain values of the order of 10^5 sec^{-1} ($\tau_{\text{CR}} \sim 10 \mu\text{sec}$!) for an rf field $H_{1S} \lesssim 10 \text{ G}$. The actual observed rates range from 10^3 to 1.0 sec^{-1} over

the same range of H_{1S} .

Molecular rotation must be taken into account. Adamantane is a very spherical molecule. The rotational activation energy is about 3 kcal/mole.^{16,17} At room temperature, the molecule jumps furiously between 24 different orientations at a jump rate¹⁶ of about $2 \times 10^{16} \text{ sec}^{-1}$. For our purposes, then, the Hamiltonian must be averaged over these orientations. The dipolar interaction coefficients A_{ik} and B_{ik} vanish in this average if the indices i and k refer to nuclei in the same molecule. Thus only intermolecular interactions need to be considered. To simplify the mathematics, the molecular rotation may be considered to be isotropic. With this model, it can be shown that the intermolecular dipolar interaction can be calculated exactly by placing all nuclei at the center of their respective molecules.¹⁸⁻²⁰ This method has been successfully used to calculate the second moment of the absorption signal in adamantane.^{17,21,22}

The calculations are thereby greatly simplified, and with the same powder-average approximation as for lithium (see Sec. IV), we obtain a correlation time²³ $\tau_C = 122 \mu\text{sec}$ using

$$\frac{1}{\tau_C^2} = \frac{16}{3} I(I+1) \gamma_I^4 \hbar^2 a_0^{-6} \langle S_1(\text{fcc}) \rangle \times [1 - \langle S_3(\text{fcc}) \rangle / \langle S_1(\text{fcc}) \rangle^2]. \quad (47)$$

As can be seen in Fig. 5, the agreement with the experimental data of Pines and Shattuck is fairly good.

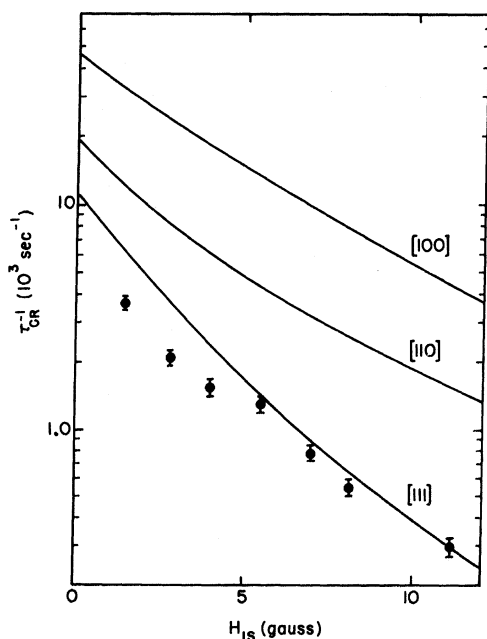


FIG. 4. Cross-relaxation rates in LiF. Data points for [111] are from Ref. 12. The solid lines are calculated from the MHW theory.

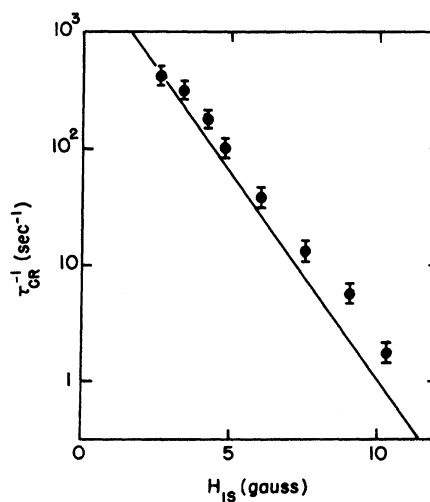


FIG. 5. Cross-relaxation rates in polycrystalline adamantane. Data points are from Ref. 4. Error bars are from A. Pines (private communication). The solid line is calculated from the MHW theory.

VI. CONCLUSION

We have shown that the MHW theory is adequate for calculating cross-relaxation rates in three cases other than CaF_2 . In each case examined, the experimentally measured rates have an exponential dependence on H_{1S} . Such a dependence has been observed in other cases also (see, for example, Ref. 5 and the comment in the reference in Ref. 4 referring to private communication with J. Waugh). This behavior leads us to conclude that, in general, very little error is generated in the calculation of cross-relaxation rates by assuming a Lorentzian correlation function—thus the MHW theory appears to be generally valid.

ACKNOWLEDGMENTS

We would like to thank Dr. D. Paquette and Dr. D. Wolf for stimulating discussions that have been very helpful in this work. Also we would like to thank Professor C. P. Slichter, Professor P. R. Moran, Dr. D. Lang, Professor A. Pines, and T. Shattuck for their cooperation and for discussions concerning their experimental work.

APPENDIX A: LATTICE SUMS

There are three different types of lattice sums necessary for computing the cross-relaxation rates in this paper. These are defined by

$$S_1 = \sum_i \left(\frac{a_0}{r_{ik}} \right)^6 [P_2(\cos\theta_{ik})]^2, \quad (\text{A1})$$

$$S_2 = \sum_i \left(\frac{a_0}{r_{ik}} \right)^{12} [P_2(\cos\theta_{ik})]^4, \quad (\text{A2})$$

and

$$S_3 = \sum_{i,j} \left(\frac{a_0}{r_{ik}} \right)^3 \left(\frac{a_0}{r_{jk}} \right)^3 \left(\frac{a_0}{r_{ij}} \right)^6 \times P_2(\cos\theta_{ik}) P_2(\cos\theta_{jk}) [P_2(\cos\theta_{ij})]^2, \quad (\text{A3})$$

where $\theta_{ik}, \theta_{jk}, \theta_{ij}$ are angles between \vec{H}_0 and $\vec{r}_{ik}, \vec{r}_{jk}, \vec{r}_{ij}$, respectively, [see Fig. 6(a)]. The lattice parameter a_0 is the distance between two nearest neighbors along the [100] direction.

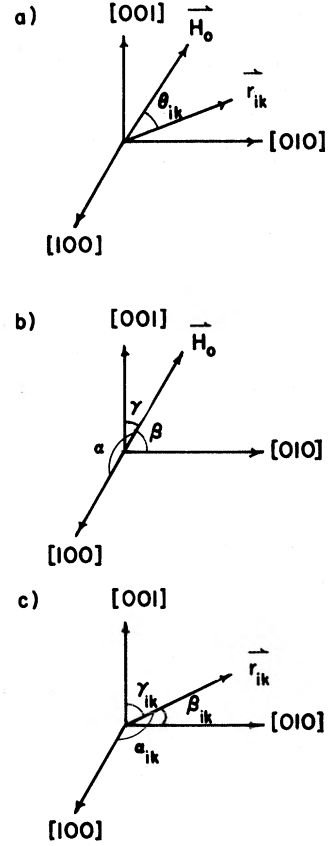


FIG. 6. Definitions of various angles used in Appendix A.

For cubic symmetric lattices, these sums can be reduced to more convenient forms by introducing the angles α, β, γ between \vec{H}_0 and the three principle axes of the crystal [see Fig. 6(b)] and the angles $\alpha_{ik}, \beta_{ik}, \gamma_{ik}$ between \vec{r}_{ik} and the three crystal axes [see Fig. 6(c)]. We then have

$$\cos\theta_{ik} = \cos\alpha \cos\alpha_{ik} + \cos\beta \cos\beta_{ik} + \cos\gamma \cos\gamma_{ik}. \quad (\text{A4})$$

Substituting this into Eqs. (A1)–(A3), we can obtain $S_1, S_2,$ and S_3 in terms of these new angles. In doing this, the following relationships proved useful:

$$\cos^2\alpha + \cos^2\beta + \cos^2\gamma = 1, \quad (\text{A5})$$

$$\cos^2\alpha \cos^2\beta + \cos^2\beta \cos^2\gamma + \cos^2\gamma \cos^2\alpha = \frac{1}{2} - \frac{1}{2}(\cos^4\alpha + \cos^4\beta + \cos^4\gamma), \quad (\text{A6})$$

$$\cos^6\alpha + \cos^6\beta + \cos^6\gamma = -\frac{1}{2} + \frac{3}{2}(\cos^4\alpha + \cos^4\beta + \cos^4\gamma) + 3 \cos^2\alpha \cos^2\beta \cos^2\gamma, \quad (\text{A7})$$

$$\begin{aligned} \cos^4\alpha \cos^2\beta + \cos^4\beta \cos^2\gamma + \cos^4\gamma \cos^2\alpha + \cos^4\alpha \cos^2\gamma \\ = \frac{1}{2} - \frac{1}{2}(\cos^4\alpha + \cos^4\beta + \cos^4\gamma) - 3 \cos^2\alpha \cos^2\beta \cos^2\gamma, \end{aligned} \quad (\text{A8})$$

$$\begin{aligned} \cos^4\alpha \cos^4\beta + \cos^4\beta \cos^4\gamma + \cos^4\gamma \cos^4\alpha \\ = \frac{1}{2} - (\cos^4\alpha + \cos^4\beta + \cos^4\gamma) - 4 \cos^2\alpha \cos^2\beta \cos^2\gamma + \frac{1}{2}(\cos^8\alpha + \cos^8\beta + \cos^8\gamma), \end{aligned} \quad (\text{A9})$$

$$\begin{aligned} & \cos^6\alpha \cos^2\beta + \cos^6\beta \cos^2\alpha + \cos^6\beta \cos^2\gamma + \cos^6\gamma \cos^2\beta + \cos^6\gamma \cos^2\alpha + \cos^6\alpha \cos^2\gamma \\ & = -\frac{1}{2} + \frac{3}{2}(\cos^4\alpha + \cos^4\beta + \cos^4\gamma) + 3\cos^2\alpha \cos^2\beta \cos^2\gamma - (\cos^8\alpha + \cos^8\beta + \cos^8\gamma), \end{aligned} \quad (\text{A10})$$

$$\cos^4\alpha \cos^2\beta \cos^2\gamma + \cos^4\beta \cos^2\gamma \cos^2\alpha + \cos^4\gamma \cos^2\alpha \cos^2\beta = \cos^2\alpha \cos^2\beta \cos^2\gamma. \quad (\text{A11})$$

In cubic lattices, α_{ik} , β_{ik} , and γ_{ik} can be cyclically rotated without changing the value of the summation. For example,

$$\sum_i \left(\frac{a_0}{r_{ik}}\right)^6 \cos^4\alpha_{ik} = \sum_i \left(\frac{a_0}{r_{ik}}\right)^6 \cos^4\beta_{ik} = \sum_i \left(\frac{a_0}{r_{ik}}\right)^6 \cos^4\gamma_{ik}. \quad (\text{A12})$$

Also, in cubic lattices, any summation involving an odd power of cosines is zero. For example,

$$\sum_i \left(\frac{a_0}{r_{ik}}\right)^6 \cos\alpha_{ik} \cos\beta_{ik} = 0. \quad (\text{A13})$$

Using these relations, we obtain the following:

$$S_1 = A_1 + B_1(\cos^4\alpha + \cos^4\beta + \cos^4\gamma), \quad (\text{A14})$$

where

$$A_1 = \frac{1}{8} \sum_i \left(\frac{a_0}{r_{ik}}\right)^6 (7 - 27\cos^4\alpha_{ik}) \quad (\text{A15})$$

and

$$B_1 = \frac{9}{8} \sum_i \left(\frac{a_0}{r_{ik}}\right)^6 (5\cos^4\alpha_{ik} - 1). \quad (\text{A16})$$

Similarly, we obtain for S_2 the following:

$$\begin{aligned} S_2 &= A_2 + B_2(\cos^4\alpha + \cos^4\beta + \cos^4\gamma) \\ &+ C_2 \cos^2\alpha \cos^2\beta \cos^2\gamma \\ &+ D_2(\cos^8\alpha + \cos^8\beta + \cos^8\gamma), \end{aligned} \quad (\text{A17})$$

where

$$A_2 = \frac{3}{32}(343A'_2 - 2322B'_2 - 2592C'_2 + 1323D'_2), \quad (\text{A18})$$

$$B_2 = \frac{1}{32}(-2322A'_2 + 15822B'_2 + 17388C'_2 - 9072D'_2), \quad (\text{A19})$$

$$C_2 = \frac{27}{8}(-72A'_2 + 483B'_2 + 602C'_2 - 273D'_2), \quad (\text{A20})$$

$$D_2 = \frac{27}{32}(49A'_2 - 336B'_2 - 364C'_2 + 195D'_2), \quad (\text{A21})$$

and

$$A'_2 = \sum_i \left(\frac{a_0}{r_{ik}}\right)^{12}, \quad (\text{A22})$$

$$B'_2 = \sum_i \left(\frac{a_0}{r_{ik}}\right)^{12} \cos^4\alpha_{ik}, \quad (\text{A23})$$

$$C'_2 = \sum_i \left(\frac{a_0}{r_{ik}}\right)^{12} \cos^2\alpha_{ik} \cos^2\beta_{ik} \cos^2\gamma_{ik}, \quad (\text{A24})$$

$$D'_2 = \sum_i \left(\frac{a_0}{r_{ik}}\right)^{12} \cos^8\alpha_{ik}. \quad (\text{A25})$$

Also, for S_3 , we get

$$\begin{aligned} S_3 &= A_3 + B_3(\cos^4\alpha + \cos^4\beta + \cos^4\gamma) \\ &+ C_3 \cos^2\alpha \cos^2\beta \cos^2\gamma \\ &+ D_3(\cos^8\alpha + \cos^8\beta + \cos^8\gamma). \end{aligned} \quad (\text{A26})$$

The expressions for A_3 , B_3 , C_3 , and D_3 are far too lengthy to be useful. A much easier procedure is to compute S_3 for four particular orientations using Eq. (A3) and, in terms of these values, compute A_3 , B_3 , C_3 , and D_3 using Eq. (A26). For example, if S_3 is computed for a powder as well as for \bar{H}_0 in the [100], [110], and [111] directions, we obtain

$$\begin{aligned} A_3 &= \frac{41}{4}S_{3,100} + 20S_{3,110} \\ &+ \frac{81}{8}S_{3,111} - \frac{315}{8}\langle S_3 \rangle, \end{aligned} \quad (\text{A27})$$

$$\begin{aligned} B_3 &= -\frac{97}{4}S_{3,100} - 44S_{3,110} \\ &- \frac{189}{8}S_{3,111} + \frac{735}{8}\langle S_3 \rangle, \end{aligned} \quad (\text{A28})$$

$$\begin{aligned} C_3 &= -\frac{147}{2}S_{3,100} - 168S_{3,110} \\ &- \frac{189}{4}S_{3,111} + \frac{1155}{4}\langle S_3 \rangle, \end{aligned} \quad (\text{A29})$$

and

$$\begin{aligned} D_3 &= 15S_{3,100} + 24S_{3,110} \\ &+ \frac{27}{2}S_{3,111} - \frac{105}{2}\langle S_3 \rangle. \end{aligned} \quad (\text{A30})$$

Computing the powder average $\langle S_3 \rangle$ is not straightforward. Consider, for example, the following term:

$$\begin{aligned} f_{ijk} &= \left(\frac{a_0}{r_{ik}}\right)^3 \left(\frac{a_0}{r_{jk}}\right)^3 \left(\frac{a_0}{r_{ij}}\right)^6 \\ &\times P_2(\cos\theta_{ik})P_2(\cos\theta_{jk})[P_2(\cos\theta_{ij})]^2. \end{aligned} \quad (\text{A31})$$

Great simplification occurs if we replace the internal angles by angles referred to an external set of axes. Since Eq. (A31) is independent of choice of external axes, let us choose the z axis to be along \hat{r}_{ij} . From the addition theorem for spherical harmonics,²⁴ we can write

$$P_2(\cos\theta_{ik}) = \frac{4}{5}\pi \sum_{m=-2}^2 Y_{2m}(\hat{r}_{ik})Y_{2m}^*(\hat{H}_0). \quad (\text{A32})$$

Using this identity, we have

$$f_{ijk} = \left(\frac{a_0}{r_{ik}}\right)^3 \left(\frac{a_0}{r_{jk}}\right)^3 \left(\frac{a_0}{r_{ij}}\right)^6 \left(\frac{4\pi}{5}\right)^3 \sum_{m_1, m_2} Y_{2m_1}(\hat{r}_{ik}) Y_{2m_2}(\hat{r}_{jk}) Y_{2m_1}^*(\hat{H}_0) Y_{2m_2}^*(\hat{H}_0) Y_{20}(\hat{H}_0) Y_{20}(\hat{H}_0). \quad (\text{A33})$$

Also, using the composition relation for spherical harmonics,²⁵ we have

$$Y_{2m_1}(\hat{H}_0) Y_{2m_2}(\hat{H}_0) = \sum_l \left(\frac{25}{4\pi(2l+1)}\right)^{1/2} \langle 2m_1 2m_2 | lm_1 + m_2 \rangle \langle 20 0 | l 0 \rangle Y_{lm_1 + m_2}(\hat{H}_0), \quad (\text{A34})$$

where $\langle 2m_1 2m_2 | lm_1 + m_2 \rangle$ and $\langle 20 0 | l 0 \rangle$ are Clebsch-Gordan coefficients.²⁶ Substitution of Eq. (A34) into Eq. (A33) gives us

$$f_{ijk} = \left(\frac{a_0}{r_{ik}}\right)^3 \left(\frac{a_0}{r_{jk}}\right)^3 \left(\frac{a_0}{r_{ij}}\right)^6 \frac{4\pi}{5} \sum_{\substack{m_1, m_2, \\ l_1, l_2}} \frac{25}{4\pi} \left(\frac{1}{(2l_1+1)(2l_2+1)}\right)^{1/2} \langle 2m_1 2m_2 | l_1 m_1 + m_2 \rangle \langle 20 0 | l_1 0 \rangle \langle 20 0 | l_2 0 \rangle^2 Y_{2m_1}(\hat{r}_{ik}) Y_{2m_2}(\hat{r}_{jk}) Y_{l_1 m_1 + m_2}^*(\hat{H}_0) Y_{l_2 0}(\hat{H}_0). \quad (\text{A35})$$

Now, we can take the powder average given by

$$\langle f_{ijk} \rangle = \frac{1}{4\pi} \int d\hat{H}_0 f_{ijk}. \quad (\text{A36})$$

Using orthonormality of spherical harmonics,

$$\int d\hat{H}_0 Y_{l_1 m_1 + m_2}^*(\hat{H}_0) Y_{l_2 0}(\hat{H}_0) = \delta_{l_1 l_2} \delta_{m_1 + m_2 0}, \quad (\text{A37})$$

and we obtain

$$\langle f_{ijk} \rangle = \left(\frac{a_0}{r_{ik}}\right)^3 \left(\frac{a_0}{r_{jk}}\right)^3 \left(\frac{a_0}{r_{ij}}\right)^6 \frac{4\pi}{5} \sum_{l, m} \frac{1}{2l+1} \langle 2m 2 - m | l 0 \rangle \langle 20 0 | l 0 \rangle^3 Y_{2m}(\hat{r}_{ik}) Y_{2-m}(\hat{r}_{jk}). \quad (\text{A38})$$

Evaluating this expression, we have

$$\langle f_{ijk} \rangle = (a_0/r_{ik})^3 (a_0/r_{jk})^3 (a_0/r_{ij})^6 \frac{3}{140} [(3 \cos^2 \theta_i - 1)(3 \cos^2 \theta_j - 1) + 4 \cos \theta_i \sin \theta_i \cos \theta_j \sin \theta_j + \sin^2 \theta_i \sin^2 \theta_j], \quad (\text{A39})$$

where θ_i, θ_j are angles between \hat{r}_{ij} (the z axis by choice) and $\hat{r}_{ik}, \hat{r}_{jk}$, respectively. Using this result, we finally have

$$\langle S_3 \rangle = \frac{3}{140} \sum_{i, j} \left(\frac{a_0}{r_{ik}}\right)^3 \left(\frac{a_0}{r_{jk}}\right)^3 \left(\frac{a_0}{r_{ij}}\right)^6 [(3 \cos^2 \theta_i - 1)(3 \cos^2 \theta_j - 1) + 4 \cos \theta_i \sin \theta_i \cos \theta_j \sin \theta_j + \sin^2 \theta_i \sin^2 \theta_j]. \quad (\text{A40})$$

For computational purposes, we can write this as

$$\langle S_3 \rangle = \frac{3}{70} a_0^{12} \sum_{i, j} r_{ik}^{-5} r_{jk}^{-5} r_{ij}^{-10} \{ [3(\hat{r}_{ik} \cdot \hat{r}_{jk})^2 - r_{ik}^2 r_{jk}^2] (r_{ik}^4 + r_{jk}^4) - 8(\hat{r}_{ik} \cdot \hat{r}_{jk})^3 (r_{ik}^2 + r_{jk}^2) + r_{ik}^4 r_{jk}^4 + 4(\hat{r}_{ik} \cdot \hat{r}_{jk})^2 r_{ik}^2 r_{jk}^2 + 7(\hat{r}_{ik} \cdot \hat{r}_{jk})^4 \}. \quad (\text{A41})$$

Table II lists computed values for S_1 , S_2 , and S_3 and associated parameters for five different cubic lattices.²⁷ Three of them, simple cubic (sc), body-centered cubic (bcc), and face-centered cubic (fcc), are straightforward with all indices referring to points on the lattice. Two of them, labeled sc' and fcc', involve lattice sums from a nonlattice point k , in particular a body-centered point.

APPENDIX B: LOCAL FIELD IN LITHIUM

The local field of ${}^7\text{Li}$ in powdered lithium metal is given by

$$H_{LI}^2 = \frac{1}{5} \gamma_I^2 \hbar^2 I(I+1) \frac{N_I}{N_I + N_S} \sum_k r_{jk}^{-6} \left[1 + \frac{4}{3} \frac{\gamma_S^2 S(S+1) N_S}{\gamma_I^2 I(I+1) N_I} + \left(\frac{\gamma_S^2 S(S+1) N_S}{\gamma_I^2 I(I+1) N_I} \right)^2 \right]. \quad (\text{B1})$$

TABLE II. Lattice sums as defined in the text of Appendix A.

	sc	sc'	bcc	fcc	fcc'
A_1	-0.8081	9.732	8.924	31.96	-83.66
B_1	4.147	-9.339	-5.192	-14.72	280.14
$S_{1,100}$	3.339	0.393	3.732	17.24	196.48
$S_{1,110}$	1.265	5.062	6.328	24.60	56.41
$S_{1,111}$	0.574	6.619	7.193	27.05	9.72
$\langle S_1 \rangle$	1.680	4.128	5.809	23.13	84.42
A_2	5.835	22.42	28.24	806	23 060
B_2	-13.899	-44.76	-58.68	-1524	-55 340
C_2	-42.367	90.34	48.06	-7483	-165 800
D_2	10.320	22.40	32.70	738	414 90
$S_{2,100}$	2.255	0.054	2.260	20.33	9216
$S_{2,110}$	0.175	2.81	2.986	136.45	579.6
$S_{2,111}$	0.0147	11.66	11.671	48.31	11.93
$\langle S_2 \rangle$	0.532	3.86	4.389	66.55	2111
A_3	2.87	29.84	48.0	646	7570
B_3	-6.32	-66.50	-94.2	-1370	-17 420
C_3	-24.04	-244.61	-381	-3050	-55 640
D_3	4.47	37.25	47.9	791	10 090
$S_{3,100}$	1.02	0.59	1.62	67.3	240
$S_{3,110}$	0.27	1.25	6.84	60.0	121.0
$S_{3,111}$	0.04	-0.002	4.24	105.8	75.8
$\langle S_3 \rangle$	0.34	0.030	3.768	58.8	-48.8

A careful evaluation of this expression, using well-known properties of lithium metal,²⁸ gives $H_{LI} = 1.17$ G at 78 °K and $H_{LI} = 1.14$ G, at 20 °C. Others^{8,29} have reported this theoretical value to be $H_{LI} = 1.20$ G, which is in slight error.

Our particular sample of lithium seemed to have a somewhat higher value of H_{LI} than the calculated value. The ratio of heat capacities ϵ can be obtained from the experimental data, using Eqs. (3) and (4). From Eq. (2) we write

$$\epsilon = \frac{1}{163} (H_{1S}/H_{LI})^2. \quad (\text{B2})$$

In Fig. 7 we plot ϵ as a function of H_{1S}^2 and obtain $H_{LI} = 1.36 \pm 0.05$ G.

To verify this result, we measured the local field using another method, that is, spin locking and then adiabatic demagnetization of H_1 to a *non-zero* value. The resulting magnetization (measured by turning off H_1 and observing the free induction decay) is given by^{8,30}

$$M = [H_{1I}/(H_{1I}^2 + H_{LI}^2)^{1/2}] M_0. \quad (\text{B3})$$

By fitting this curve to experimental points (see

$$\int_{-\infty}^{\infty} g_{jj'}(\omega)(\omega^2 - \Omega_I^2) d\omega = \frac{1}{\hbar^2} \frac{1}{4} \left[\frac{1}{3} I(I+1) \right]^2 (2I+1)^{N_I} \left(\sum_{k,p} 5 B_{jk} B_{j'k} A_{kp}^2 + \sum_{k,k'} 4 B_{jk} B_{j'k'} A_{kk'}^2 \right). \quad (\text{C1})$$

Eqs. (A25), (A26), and (A28) in LS consequently are also in error, and Eq. (A29) in LS should finally be

$$\frac{1}{T_{IS}} = \left(1 + \frac{N_S S(S+1) \gamma_S^2 (H_{1S})^2}{N_I I(I+1) \gamma_I^2 [(H_{1I})^2 + \frac{1}{3} \langle \Delta^2 H \rangle_{II}]} \right) \frac{4}{3} \frac{\gamma_S^2}{\gamma_I^2} \left(\frac{\pi \langle \Delta^2 \omega \rangle_{II}}{10K'} \right)^{1/2} e^{-(\Omega_S - \Omega_I)^2 / \omega_1^2}, \quad (\text{C2})$$

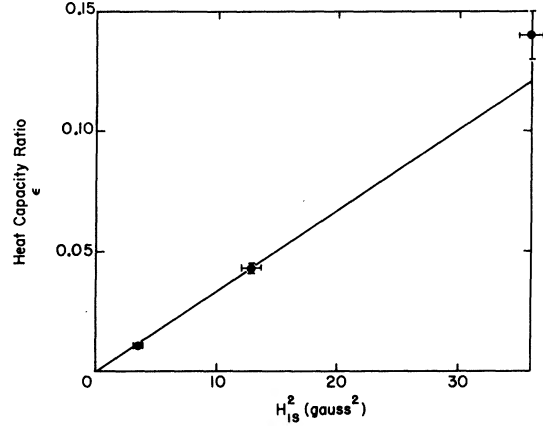


FIG. 7. Measured ratio of heat capacities as a function of H_{1S} . The straight line shown is the best fit through the three data points and the origin.

Fig. 8), we obtain $H_{LI} = 1.55 \pm 0.10$ G.

Although this value for the local field is somewhat higher than the value obtained from cross-relaxation data, the data in Fig. 8 is particularly sensitive to small nonadiabatic effects in the demagnetization which would cause the local field to appear larger than its true value. Our results do verify the fact that the local field in our sample is indeed significantly larger than the theoretical value. This appears to be a peculiarity of our sample, perhaps due to a small quadrupolar interaction with crystal defects and impurities. Other published data seem to also show this effect (see Appendix C).

APPENDIX C: LURIE-SLICHTER EXPERIMENT

In 1964 Lurie and Slichter²⁹ (LS) published experimental results for lithium metal ($I = {}^7\text{Li}; S = {}^6\text{Li}$) which demonstrated the validity of spin temperature concepts in nuclear double resonance. They used a pulse sequence identical to that described in this paper [see Fig. 1(a)]. This affords us an excellent opportunity to compare their data with the MHW theory, using Eqs. (22) and (37).

In the Appendix of LS, a calculation of the cross-relaxation rate was presented and then applied to the experimental data, using an equation equivalent to Eq. (37). We found some minor errors in that treatment which we would like to report here.

Equation (A24) in LS should be

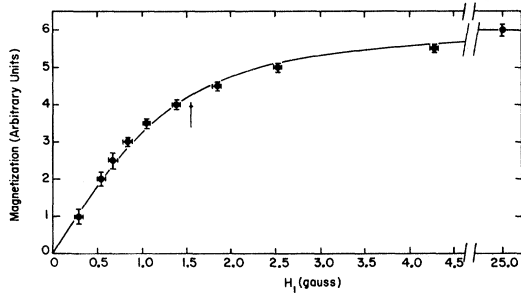


FIG. 8. Magnetization following an adiabatic demagnetization of the rf field to a value H_{II} . From this data, the local field of ${}^7\text{Li}$ was determined to be $H_{LI} = 1.55 \pm 0.10$ G, shown by the arrow in the figure. The solid line shown is obtained from Eq. (B3) using this value for H_{LI} .

where

$$\omega_1^2 = \frac{5}{18} \langle \Delta^2 \omega \rangle_{II} K', \quad (\text{C3})$$

and

$$K' = \left(\sum_{i,j} A_{ij}^2 (B_{jm}^2 + \frac{4}{5} B_{im} B_{jm}) \right) / \left(\sum_j A_{ij}^2 \right) \left(\sum_j B_{jm}^2 \right). \quad (\text{C4})$$

Similarly, Eq. (A31) in LS should be

$$\frac{1}{T_{IS}^{-1}} = \left(1 + \frac{N_S \gamma_S^2 S(S+1) (H_1)_S^2}{N_I \gamma_I^2 I(I+1) \frac{1}{3} \langle \Delta^2 H \rangle_{II}} \right) \times \frac{2}{3} \frac{\gamma_S^2}{\gamma_I^2} \left(\frac{\pi \langle \Delta^2 \omega \rangle_{II}}{K} \right)^{1/2} e^{-\alpha_S^2 / \omega_1^2}, \quad (\text{C5})$$

where

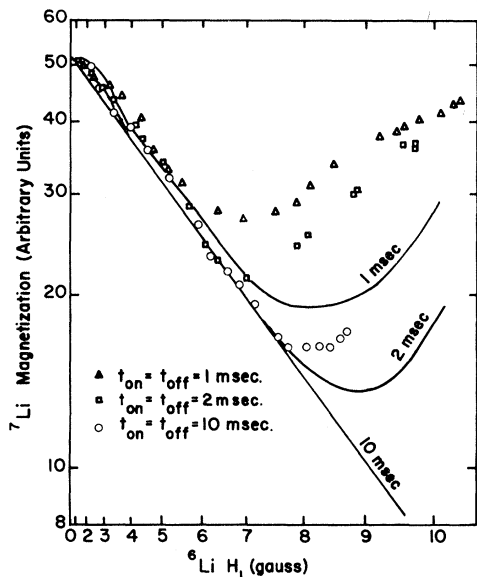


FIG. 9. Correction of Fig. 9 in LS (Ref. 29) using Eq. (C2) in this paper instead of Eq. (A29) in LS.

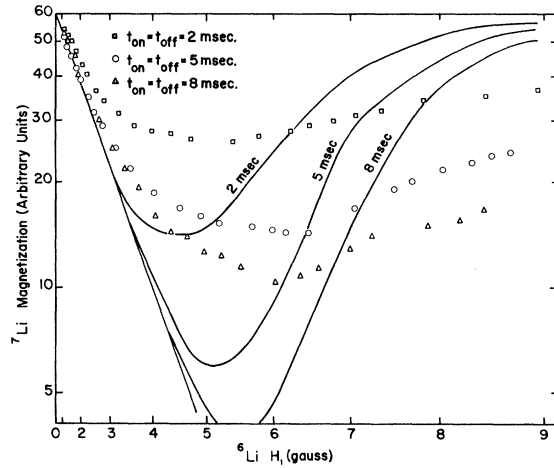


FIG. 10. Correction of Fig. 10 in LS (Ref. 29) using Eq. (C5) in this paper instead of Eq. (A31) in LS.

$$\omega_1^2 = \frac{4}{9} \langle \Delta^2 \omega \rangle_{II} K, \quad (\text{C6})$$

and K is defined by Eq. (27) in this paper.

The theoretical lines in Figs. 9 and 10 in LS were also drawn wrong, even if Eqs. (A29) and (A31) in LS were used as written. It appears that T_{IS}^{-1} was evaluated wrong using a factor which was 2π too small. This could be due possibly to the use of the wrong units for γ_I and γ_S . Accordingly, in Figs. 9 and 10 of this paper, the solid curves represent the corrected theory of Eqs. (C2) and (C5) above. The data on these figures is redrawn from Figs. 9 and 10 of LS.

The corrected result, as given in Eq. (C5), is identical to what we would obtain from Eqs. (12) and (13) if we had assumed the form of $G(\tau)$ to be Gaussian.

$$G(\tau) = e^{-\tau^2 / \tau_C^2}. \quad (\text{C7})$$

As can be seen in Fig. 10, the agreement between data and theory is not very good in this case. If

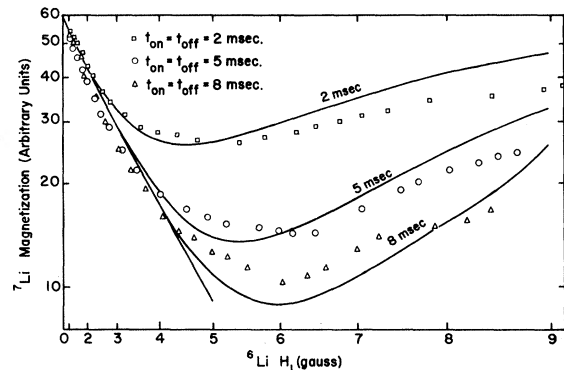


FIG. 11. M_I vs H_{1S} in lithium metal for $N=25$. The data points are from Ref. 29. The solid line is calculated from the MHW theory and Eq. (31) using $H_{LI} = 1.4$ G.

we apply the MHW theory [which assumes $G(\tau)$ to be Lorentzian instead of Gaussian], the agreement between data and theory is not significantly improved. If, however, we use a local field $H_{LI}=1.4$ instead of 1.2 G, the agreement is much better (see Fig. 11). This seems to indicate that the local field in their sample of lithium is larger than the

calculated dipolar local field, just as we observed in our sample (see Appendix B). LS also made an independent measurement of the local field by a method identical to that described in Fig. 8 of this paper and determined H_{LI} to be 1.2 G. We do not know the source of this apparent discrepancy.

*Research supported by the U.S. NSF under Grant No. GH31671.

- ¹D. A. McArthur, E. L. Hahn, and R. E. Walstedt, *Phys. Rev.* **188**, 609 (1969).
- ²D. E. Demco, J. Tegenfeldt, and J. S. Waugh, *Phys. Rev. B* **11**, 4133 (1975).
- ³In MHW, this term is written with the subscript indices reversed, contrary to the convention employed in DTW (Ref. 2) and also in this paper.
- ⁴A. Pines and T. W. Shattuck, *J. Chem. Phys.* **61**, 1255 (1974).
- ⁵M. Mehring, H. Raber, and G. Simning, 18th Ampere Congress, Nottingham, 1974, p. 35 (unpublished).
- ⁶A. G. Anderson and S. R. Hartmann, *Phys. Rev.* **128**, 2023 (1962).
- ⁷J. R. Franz and C. P. Slichter, *Phys. Rev.* **148**, 287 (1966).
- ⁸D. C. Ailion and C. P. Slichter, *Phys. Rev.* **137**, A235 (1965).
- ⁹D. Wolf, *J. Magn. Reson.* **17**, 1 (1975).
- ¹⁰D. Wolf, *Phys. Rev. B* **10**, 2710 (1974).
- ¹¹D. Wolf, *Phys. Rev. B* **10**, 2724 (1974).
- ¹²D. V. Lang and P. R. Moran, *Phys. Rev. B* **1**, 53 (1970).
- ¹³M. E. Zhabotinskii, A. E. Mefed, and M. I. Rodak, *Zh. Eksp. Teor. Fiz.* **61**, 1917 (1971) [*Sov. Phys.-JETP* **34**, 1020 (1972)].
- ¹⁴H. T. Stokes and D. C. Ailion (unpublished).
- ¹⁵C. E. Nordman and D. L. Schmitkons, *Acta Crystallogr.* **18**, 764 (1965).
- ¹⁶H. A. Resing, *Mol. Cryst.* **9**, 101 (1969).
- ¹⁷J. D. Graham and J. K. Choi, *J. Chem. Phys.* **62**, 2509 (1975).
- ¹⁸G. W. Smith, *J. Chem. Phys.* **36**, 3081 (1962).
- ¹⁹L. V. Dmitrieva and V. V. Moskalev, *Fiz. Tverd. Tela* **5**, 2230 (1963) [*Sov. Phys.-Solid State* **5**, 1623 (1964)].
- ²⁰D. J. Kroon, *Philips Res. Rep.* **15**, 501 (1960).
- ²¹D. W. McCall and D. C. Douglass, *J. Chem. Phys.* **33**, 777 (1960).
- ²²G. W. Smith, *J. Chem. Phys.* **35**, 1134 (1961).
- ²³A. Pines and T. W. Shattuck (private communication) first made this calculation and obtained precisely the same value for τ_C as did we.
- ²⁴Albert Messiah, *Quantum Mechanics* (Wiley, New York, 1958), Vol. II, p. 1074.
- ²⁵See Ref. 24, p. 1057.
- ²⁶John C. Slater, *Quantum Theory of Atomic Structure* (McGraw-Hill, New York, 1960), Vol. II, pp. 93-94.
- ²⁷In DTW, Table I and Eqs. (3.15)-(3.18) are inconsistent with Eq. (2.11). The lattice sums S_2 and S_4 are too large by a factor of 9, and the lattice sums S_3 and S_5 through S_{12} are too large by a factor of 81. This was compensated by reducing the right-hand side of Eqs. (3.15) and (3.17) by a factor of 9 and Eqs. (3.16) and (3.18) by a factor of 81. Thus, the two errors cancel each other, giving the correct results. Also note that Eq. (3.15) contains a typographical error. It should read
- $$M_2 = \frac{1}{27} 2I(I+1)(S_1 S_2 - 2S_4)/S_1.$$
- These corrections will eliminate discrepancies between DTW and this paper.
- ²⁸Jerry Donohue, *The Structures of the Elements* (Wiley, New York, 1974), pp. 28-30.
- ²⁹F. M. Lurie and C. P. Slichter, *Phys. Rev.* **133**, A1108 (1964).
- ³⁰C. P. Slichter and W. C. Holton, *Phys. Rev.* **122**, 1701 (1961).